Spin-excited oscillations in two-component fermion condensates

Tomoyuki Maruyama[1,2,3] and George F. Bertsch[1]
[1]*Institute for Nuclear Theory, University of Washington, Seattle, Washington 98195, USA*
[2]*College of Bioresource Sciences, Nihon University, Fujisawa 252-8510, Japan*
[3]*Advanced Science Research Center, Japan Atomic Energy Research Institute, Tokai 319-1195, Japan*
(Received 5 March 2005; published 12 January 2006)

We investigate collective spin excitations in two-component fermion condensates with special consideration of unequal populations of the two components. The frequencies of monopole and dipole modes are calculated using Thomas-Fermi theory and the scaling approximation. As the fermion-fermion coupling is varied, the system shows various phases of the spin configuration. We demonstrate that spin oscillations have more sensitivity to the spin phase structures than the density oscillations.

DOI: 10.1103/PhysRevA.73.013610 PACS number(s): 03.75.Ss, 32.80.Pj, 05.30.Fk, 67.57.Jj

I. INTRODUCTION

Since the realization of the Bose-Einstein condensed (BEC) atomic gases [1,2], there has been much interest in ultracold trapped atomic systems to study quantum many-body phenomena. Besides the Bose-Einstein condensates (BEC) [1–3], one can now study degenerate atomic Fermi gases [4] and Bose-Fermi mixtures [5]. These systems offer great promise to exhibit new and interesting phenomena of quantum many-particle physics. An important diagnostic signal for these systems is the spectrum of collective excitations. Such oscillations are common to a variety of many-particle systems and are often sensitive to the interaction and the structure of the ground state.

However, for harmonically trapped gases of either bosonic or fermionic atoms, the frequencies of the density oscillations are quite insensitive to the strength of the interaction. In particular, the dipole oscillation frequency is completely independent of the interaction [6]. As we will see, excitations where the two components move out of phase (spin excitations) behave quite differently.

The underlying theoretical tool to treat dynamic problems of dilute quantum gases is the time-dependent mean field theory. This is reduced to the random-phase approximation (RPA) for small amplitudes, and the theory in this form has been applied to density oscillations of these systems [7–9]. When the single-particle spectrum is regular, the long-wavelength excitations are collective and simpler methods can be used to calculate the frequencies, in particular with sum rules [10] or the scaling approximation [11–13]. In this work we will follow the last approach, which we believe is justified by the extreme regularity of the harmonic trapping potential. The scaling method is physically quite transparent, but it is in fact equivalent to the theory based on energy-weighted sum rules [12], as used for example in Ref. [10].

In the dilute limit, the interaction in a two-component fermion condensate is characterized by a single number, the scattering length a. We will only consider here the case of positive scattering lengths which correspond to a repulsive interaction. When the interaction is attractive, the system is superfluid in its ground state and the excitation properties are controlled by the energy gap.

The ground state properties of the two-component fermion system with a repulsive interaction was treated by Sogo and Yabu [14], who showed that there are three regimes, depending on the interaction strength. For small interaction strengths, the ground state has equal densities of the two components, which we call the "paramagnetic" regime. Beyond a certain threshold in interaction strength, the ground state becomes "ferromagnetic," that is with unequal densities of the two components. At very large interaction strengths, the minority component vanishes. We shall call this the single-component phase. In this work, we will treat systems in the presence of an external magnetic field, which will produce a net spin in the ground state even in the paramagnetic regime.

We now briefly describe the spin modes that could be excited by a time-dependent external magnetic field. The simplest field to consider is one that is spatially uniform. However, such fields cannot change the spatial part of the single-particle wave functions of the condensate and do not induce internal excitations. The response to a uniform field is identical to that of a noninteracting ensemble of N_1-N_2 atoms, where N_i is the number of atoms in component i. The next field to consider has a dipole spatial dependence. Due to the constraints of Maxwell's equations, the overall multipolarity of such a field is $J=2$, but we shall follow the common terminology calling it dipole. The spin-dipole mode has been discussed previously in Refs. [7,10]. Reference [10] treats the spin dipole mode as overdamped in the hydrodynamical region and does not discuss its frequency at zero temperature. In Ref. [7], the spin dipole response was calculated in RPA for a particular value of the coupling strength, and it was found to be rather narrow and close to the unperturbed oscillation frequency.

The JILA group [15] performed experiments of the dipole oscillation in two-component fermions with different trapped frequencies above the Fermi temperature. In these experiments they observed oscillation frequencies and damping times as functions of the fermion-fermion coupling, and succeeded to show the transition from the collisionless regime to the hydrodynamical regime. In addition the JILA group also showed that the damping effect becomes smaller as the temperature decreases [16]. At zero temperature most of the collisions between two fermions are suppressed by the Pauli blocking, and the damping of the mode should not be taken into consideration. Thus we can expect to see the spin phase

 ©2006 The American Physical Society

structures by investigating the spin excited oscillations. In our work here, we will calculate the frequency by changing the coupling strength and the external static magnetic field.

II. GROUND STATE

We begin with the expression for the energy of a dilute trapped condensate in the mean-field approximation,

$$E_T = \int d^3r \left(-\frac{\hbar^2}{2m} \sum_n^{\text{occ}} \sum_{s=1,2} \psi_{ns}^* \nabla^2 \psi_{ns} + \frac{m}{2}(\Omega_T^2 r_1^2 + \Omega_T^2 r_2^2 + \Omega_L^2 r_3^2) \times (\rho_1 + \rho_2) + g\rho_1\rho_2 - B(\mu\rho_1 - \mu\rho_2) \right). \quad (1)$$

Here ψ_{ns} are orbital wave functions indexed by spin $s=1,2$, $\Omega_{L,T}$ are the longitudinal and transverse frequencies of the trapping field, g is the coupling strength of a contact interaction, μ is the magnetic moment of the atoms, and B is an external magnetic field. The densities ρ_s are given by the usual sum over occupied orbitals, $\rho_s = \Sigma_n^{\text{occ}} |\psi_{n,s}|^2$.

We shall use the Thomas-Fermi approximation to evaluate the first term, the kinetic energy. We can then make a change of variables to simplify the appearance of the Thomas-Fermi equations, similar to the scaling defined in Ref. [14]. With the scaled variables and the Thomas-Fermi approximation, the expression for the energy is, up to an additive constant,

$$\tilde{E}_T = \int d^3x \left[\sum_{i=1,2} \left(\frac{3}{5} n_i^{5/3} + x^2 n_i \right) + g n_1 n_2 - \tilde{B}(n_1 - n_2) \right], \quad (2)$$

where $x^2 = |\mathbf{x}|^2$. Here the variables are defined

$$x_j = \left(\frac{m^2 \Omega_j}{3\pi^2 \hbar^3} \right) r_j \quad (j = 1-3),$$

$$n_i = \left(\frac{m}{\hbar^2} \right)^3 \frac{2}{9\pi^4} \rho_i \quad (i = 1,2),$$

$$\tilde{B} = \left(\frac{m}{\hbar^2} \right)^3 \frac{2}{9\pi^4} B\mu,$$

$$\tilde{E}_T = \frac{4m^{12} \Omega_L \Omega_T^2}{(3\pi^2)^7 \hbar^{21}} E_T. \quad (3)$$

The TF equations for the densities $n_{1,2}$ are derived by variation of the energy (3) with a constraint on the total number of particles. This yields

$$n_1^{2/3} + g n_2 = e_f - x^2 + \tilde{B},$$

$$n_2^{2/3} + g n_1 = e_f - x^2 - \tilde{B}. \quad (4)$$

In this equation the Lagrange multiplier e_f has the meaning of the Fermi energy. The solution of these equations in the absence of a magnetic field is discussed in detail in Ref. [14]. Those authors make an additional rescaling to eliminate g, but we do not do that here. For any positive g, there is a value of e_f above which the system becomes ferromagnetic. At $g=1$, the critical point is at $e_f = 20/27$.[1] Below that value, the minimum energy is obtained for the paramagnetic phase, having $n_1 = n_2$. Just above that value, both components are present but the densities are unequal. When e_f is increased past $e_f = 1$, the system goes into a single-component phase in the center of the trap, at $x=0$. Away from the center of the trap, the Fermi energy is effectively reduced, allowing the paramagnetic phase to persist in the outer part of the condensate cloud. Thus the minority component will form a hollow sphere, which we will call the hollow spin phase.

Here we would like to give a comment. In Eq. (1) we assume that the magnetic moments of the two sorts of atoms are equal in magnitude and opposite in sign. The derivation of Eqs. (4) does not need this assumption; we can obtain the same equations by changing the definitions of variables e_f and $\tilde{B}$. In this generalization, however, e_f and $\tilde{B}$ are not proportional to the actual Fermi energy and the external magnetic field, respectively. It is not easy to interpret the physical meanings of these variables, and so we disregard this generalization here.

Now consider the effect of a magnetic field. If $\tilde{B} \neq 0$, the densities $n_{1,2}$ will be unequal no matter what the value of g. Still, one can distinguish two kinds of behavior near the center of the trap. If the densities of both spins decrease as one moves away from the center, we shall call it paramagnetic. However, for a certain range of parameters, the density of the minority component may increase initially, moving away from the center. This is the ferromagnetic phase. The system can also form the hollow spin phases in the presence of a magnetic field. When the external magnetic field $\tilde{B}$ increases more, the minority component disappears completely, giving what we call the single-spin phase.

Density profiles illustrating these three regimes are shown in Fig. 1. The panels show the densities as a function of distance x in a weak magnetic field ($g^2\tilde{B} = 1.0 \times 10^{-4}$) and at three different interaction strengths, $g=0.95$ (a), 1.05 (b) and 1.15 (c). From top to bottom, the panels show paramagnetic (a), ferromagnetic (b), and the hollow spin phases (c). The solid and dashed lines represent the scaled density distribution of major and minor components of fermions.

The phase boundaries as functions of $\tilde{B}$ and g are shown in Fig. 2. The upper and lower columns show the same results, but in the lower column the vertical line is rescaled by factor g^2.

The dashed line represents the border between the paramagnetic and ferromagnetic phases, which is given by $\partial^2 n_2(x)/\partial x^2 = 0$ at $x=0$.

The solid line represents the results solved by $n_2(0) = 0$ in Eq. (4). This line crosses the dashed line at $g = 1/\sqrt{2}$ and $g^2\tilde{B} = 1/27$. The curvature of the minority component density, $\partial^2 n_2(x)/\partial x^2$ at $x=0$, is negative when $g < 1/\sqrt{2}$ and positive when $g > 1/\sqrt{2}$. This solid line shows the border be-

[1] The scattering length at this critical point depends on the trapped frequency, the fermion mass, and the fermion number, and the actual value as for ^{40}K was discussed in Ref. [14].

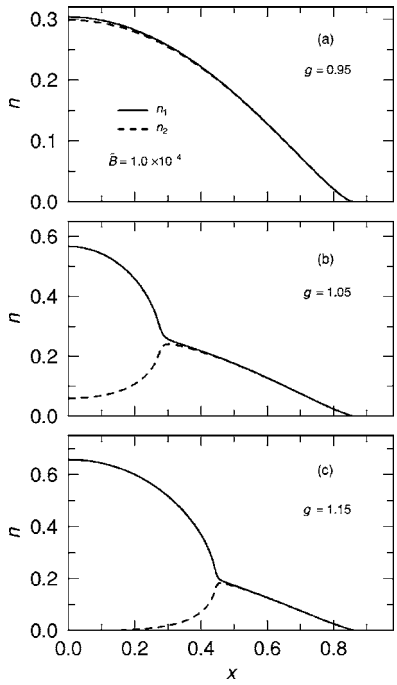

FIG. 1. The scaled density distribution of two components fermion at $g=0.95$ (a), $g=1.05$ (b), and $g=1.15$ (c) with $e_f=20/27$ and $g^2\tilde{B}=1.0\times10^{-4}$. The solid and dashed lines represent the distribution of the major and minor components, respectively.

tween the single and paramagnetic spin phases when $g<1/\sqrt{2}$, and the border between the ferromagnetic and hollow spin phases when $g>1/\sqrt{2}$.

In the hollow phases there are two boundaries for the minority fermion density where $n_2=0$ and $n_1\neq0$. On this boundary the density of majority fermion must satisfy

$$n_1^{2/3}-gn_1=2\tilde{B}. \tag{5}$$

Here we should consider the following function:

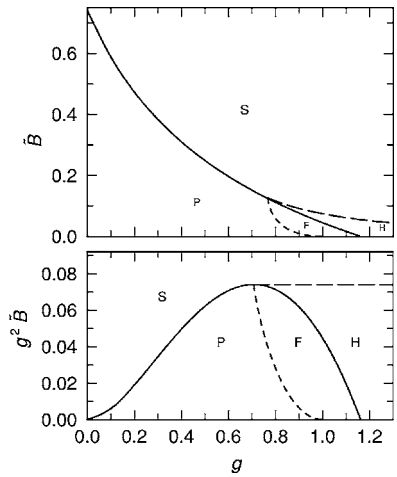

FIG. 2. The phase diagram of the two components of the fermion. The symbols "*S*," "*P*," "*F*," and "*H*" denote the region of the single-component, paramagnetic, ferromagnetic, single, and hollow phases.

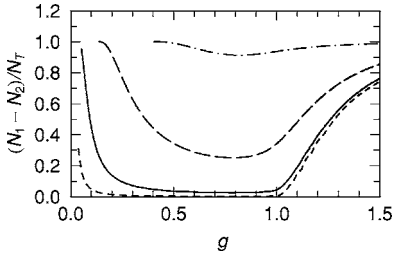

FIG. 3. The asymmetry of the two components as a function of the coupling constant g, at $e_f=20/27$. The dashed, solid, long-dashed, and dotted lines represent the results with the external magnetic fields $g^2\tilde{B}=1.0\times10^{-4}$, 1.0×10^{-3}, 1.0×10^{-2}, and 5.0×10^{-2}, respectively.

$$f(n)=n^{2/3}-gn-2\tilde{B}. \tag{6}$$

The derivative of the above equation is

$$\frac{d}{dn}f(n)=f'(n)=\frac{2}{3}n^{-1/3}-g. \tag{7}$$

Since $f'(8/27g^3)=0$, $f(0)=f(1/g^3)=-2B<0$, and $f'(1/g^3)<0$, $f(n)$ becomes maximum at $n=8/27g^3$. Thus $f(8/27g^3)>0$ is required, otherwise $f(n)\leqslant0$, and there is no boundary of n_2, which means $n_2=0$ in all regions. From that we can obtain the condition for $\tilde{B}$ as

$$\tilde{B}<\tilde{B}_{\max}=\frac{1}{2}\left(\frac{4}{9g^2}-\frac{8}{27g^2}\right)=\frac{2}{27g^2}\approx0.074g^{-2}. \tag{8}$$

The long-dashed line represents $\tilde{B}=2/27g^{-2}\approx0.074g^{-2}$ for $g>1/\sqrt{2}$, which means the border between the hollow and single spin phases.

In Fig. 3 we plot the number asymmetry between two components $(N_1-N_2)/N_T$, where $N_T=N_1+N_2$. When the external magnetic field is small, the asymmetry of the fermion number is very small and almost independent of the coupling in the paramagnetic phase ($g\lesssim1.0$) except when the coupling is very small, where the system is close to the border between the paramagnetic and single spin phases. As the coupling increases further and exceeds about $g\approx1.0$, the system is changed from the paramagnetic spin phase to the ferromagnetic one. The number asymmetry of the fermion number also increases.

As the external magnetic field becomes larger, the change of the number asymmetry is not drastic, though the rapid change of the dipole frequency still remains.

With fixed values of e_f and $g^2\tilde{B}$, the spin phase of the two component Fermi gas turns to be paramagnetic, ferromagnetic, and hollow in order as the coupling constant, g, increases. In the following sections we calculate the frequencies of collective oscillations in the same conditions and discuss relations between their frequencies and the phases.

III. DIPOLE EXCITATIONS

In this section we derive an expression for the dipole frequency using the scaling method. Without loss of generality,

we take the direction of motion along the z axis. The time-varying density will be parametrized with a collective coordinate λ_i as [11]

$$\rho_i(\mathbf{r}) = \rho_i^{(0)}(r_1, r_2, r_3 - \lambda_i), \tag{9}$$

where $\rho_i^{(0)}(\mathbf{r})$ is the density distribution of the ground state. Substituting Eq. (9) into Eq. (1), we can obtain the variation of the total energy up to the order of $O(\lambda^2)$ as

$$\Delta E_T = E_T - E_T^{(0)} \approx -\tfrac{1}{2} m\Omega_L^2(\lambda_1^2 N_1 + \lambda_2^2 N_2) + A(2\lambda_1\lambda_2 - \lambda_1^2 - \lambda_1^2), \tag{10}$$

where $\tilde{E}_T^{(0)}$ is the ground state energy ($\lambda_i = 0$), and

$$A = \frac{g}{2}\int d^3 r \frac{\partial \rho_1^{(0)}}{\partial z}\frac{\partial \rho_2^{(0)}}{\partial z}. \tag{11}$$

When we consider the time dependence of λ_i, the mass parameter with respect to λ_i is obtained as mN_i [11].

Then the classical equation of motion for $\boldsymbol{\lambda}$ is harmonic, giving rise to the following eigenvalue equation for the oscillation frequencies:

$$\begin{pmatrix} m(\Omega_L^2 - \omega^2)N_1 - 2A & 2A \\ 2A & m(\Omega_L^2 - \omega^2)N_2 - 2A \end{pmatrix}\begin{pmatrix} \lambda_1 \\ \lambda_2 \end{pmatrix} = 0. \tag{12}$$

The eigenvalues of this equation are given as

$$\omega^2 = \Omega_L^2 - \left(\frac{A}{mN_1} + \frac{A}{mN_2}\right) \pm \left(\frac{A}{mN_1} + \frac{A}{mN_2}\right). \tag{13}$$

One eigenvalue is $\omega = \Omega_L$ with the eigenvector $\lambda_1 = \lambda_2$. This is the in-phase oscillation of the system which follows Kohn's theorem.

The other eigenvalue is

$$\omega = \omega_D \equiv \left[\Omega_L^2 - \left(\frac{2A}{mN_1} + \frac{2A}{mN_2}\right)\right]^{1/2}. \tag{14}$$

The eigenvector is given by $\lambda_1/N_1 = -\lambda_2/N_2$. In this mode, the two components move in opposite directions keeping their center of mass at rest.

Here we should give a comment. If we consider the dipole oscillation in the transverse relation, the frequency normalized by the transverse trapped frequency ω_D/Ω_T is also equivalent to the right-hand side of Eq. (14).

Using the variable transformation explained in the preceding sections, the dipole frequency is written as

$$\omega_D/\Omega_{L(T)} = \left[1 - \tilde{A}\left(\frac{1}{\tilde{N}_1} + \frac{1}{\tilde{N}_2}\right)\right]^{1/2}, \tag{15}$$

where

$$\tilde{A} = \frac{g}{6}\int d^3 x \frac{\partial n_1}{\partial x}\frac{\partial n_2}{\partial x}, \tag{16}$$

$$\tilde{N}_i = \int d^3 x n_i = \frac{2m^9}{3^5 \pi^{10}\hbar^{15}} N_i. \tag{17}$$

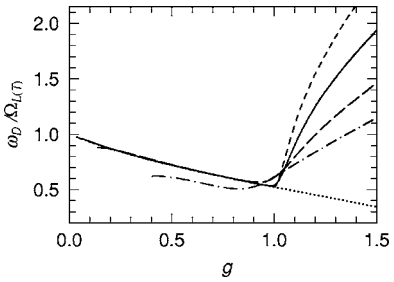

FIG. 4. The frequencies of the dipole oscillations as a function of the coupling constant g. The dashed, solid, long-dashed, and dotted lines represent the results with the external magnetic fields $g^2\tilde{B} = 1.0\times10^{-4}$, 1.0×10^{-3}, 1.0×10^{-2}, and 5.0×10^{-2}, respectively. The dotted line denotes the result of the symmetric system.

In Fig. 4 we show the frequency of the dipole oscillation in the out-of-phase oscillation as a function of the coupling constant, g, with various external magnetic fields, $g^2\tilde{B} = 1.0\times10^{-4}$ (dashed), 1.0×10^{-3} (solid), 1.0×10^{-2} (long-dashed), and 5.0×10^{-2} (chain-dotted), respectively. For comparison we also show the frequencies in the symmetric system in zero magnetic field (dotted line).

As the coupling becomes larger, the dipole frequency decreases monotonically until $g \approx 1.0$, and sharply increases above that. For $g \lesssim 1.0$, where the number asymmetry is small, the frequency ω_D does not strongly depend on the external magnetic field. In the paramagnetic spin phase ($g \lesssim 1$), the density distribution of the minor component of fermion n_2 is similar to that of the major component n_1, and the integrand in $\tilde{A} > 0$ (16) is positive in all regions. As the coupling increases, the size of the Fermi gas becomes larger, and then the frequency ω_D monotonously decreases.

As the coupling becomes $g \gtrsim 1$ one component of the fermions is partially converted into the other component, and ferromagnetism appears in the central region. In Fig. 1(b) $\partial n_2/\partial x > 0$ for $x < x_c$ and $\partial n_2/\partial x < 0$ for $x > x_c$, where $x_c \approx 0.32$; namely there is a ferromagnetic region for $x < x_c$. The contribution from this ferromagnetic region to $\tilde{A}$ is negative. As the coupling increases, the critical position x_c moves to the surface, $\tilde{A}$ becomes smaller, and then ω_D increases.

In the case of a strong magnetic field, the qualitative behavior is similar. In strong coupling $g \gtrsim 1$ the slope of the density function for the minor fermion n_2 is smaller in the strong magnetic field than that in the weak magnetic field. As the external magnetic field increases, the dipole frequency becomes smaller.

IV. MONOPOLE OSCILLATION

In this section we study the monopole oscillation in spherical trap, $\Omega_T = \Omega_L = \Omega_M$. Generally the monopole and quadrupole oscillations are coupled, but qualitative properties do not have significant difference between the two collective oscillations. In order to study the monopole oscillation, we introduce the following scaling:

$$\rho_i(\mathbf{r}) = e^{3\lambda_i}\rho_i^{(0)}(e^{\lambda_i}\mathbf{r}). \tag{18}$$

Under this scaling the total energy becomes

$$E_T = \sum_{i=1,2} (e^{2\lambda_i} T_i + e^{-2\lambda_i} U_i) + V_{12}, \tag{19}$$

where the T_i and U_i are the kinetic and harmonic oscillator energy parts in the ground state, respectively. The interaction energy V_{12} appears

$$\begin{aligned} V_{12} &= g e^{3\lambda_1+3\lambda_2} \int d^3 r \rho_1^{(0)}(e^{\lambda_1}\mathbf{r}) \rho_2^{(0)}(e^{\lambda_2}\mathbf{r}) \\ &\approx -g \int d^3 r \left(\lambda_1 \rho_1^{(0)} \mathbf{r} \frac{\partial \rho_2^{(0)}}{\partial \mathbf{r}} + \lambda_2 \mathbf{r} \frac{\partial \rho_1^{(0)}}{\partial \mathbf{r}} \rho_2^{(0)} \right) \\ &\quad + K_{11}\lambda_1^2 + K_{22}\lambda_2^2 + 2K_{12}\lambda_1\lambda_2 \end{aligned} \tag{20}$$

with

$$K_{11} = -\frac{g}{2} \int d^3 r \left[\left(3 + \mathbf{r} \frac{\partial}{\partial \mathbf{r}} \right) \rho_1^{(0)} \right] \left(\mathbf{r} \frac{\partial}{\partial \mathbf{r}} \rho_2^{(0)} \right), \tag{21}$$

$$K_{22} = -\frac{g}{2} \int d^3 r \left(\mathbf{r} \frac{\partial}{\partial \mathbf{r}} \rho_1^{(0)} \right) \left[\left(3 + \mathbf{r} \frac{\partial}{\partial \mathbf{r}} \right) \rho_2^{(0)} \right], \tag{22}$$

$$K_{12} = \frac{g}{2} \int d^3 r \left[\left(3 + \mathbf{r} \frac{\partial}{\partial \mathbf{r}} \right) \rho_1^{(0)} \right] \left[\left(3 + \mathbf{r} \frac{\partial}{\partial \mathbf{r}} \right) \rho_2^{(0)} \right]. \tag{23}$$

The mass parameter of the monopole oscillation is given by the mass times the mean square radius. Then the monopole oscillation mode and frequencies ω_M are obtained by

$$(B_M \omega^2 - C_M)\boldsymbol{\lambda} = 0 \tag{24}$$

with

$$B_M = \frac{m}{2} \begin{pmatrix} X_1 & 0 \\ 0 & X_2 \end{pmatrix}, \tag{25}$$

$$\mathcal{C}_M = \begin{pmatrix} C_{11} & K_{12} \\ K_{12} & C_{22} \end{pmatrix} = \begin{pmatrix} 2T_1 + 2U_1 + K_{11} & K_{12} \\ K_{12} & 2T_2 + 2U_2 + K_{22} \end{pmatrix}, \tag{26}$$

where

$$X_i = \int d^3 r \rho_i(\mathbf{r}) \mathbf{r}^2. \tag{27}$$

Using the variable transformation explained in Sec. II,

$$\left[\left(\frac{\omega_M}{\Omega_M} \right)^2 \tilde{B}_M - \tilde{C}_M \right] \boldsymbol{\lambda} = 0 \tag{28}$$

with

$$\tilde{B}_M = \begin{pmatrix} \tilde{X}_1 & 0 \\ 0 & \tilde{X}_2 \end{pmatrix}, \tag{29}$$

$$\tilde{C}_M = \begin{pmatrix} 2\tilde{T}_1 + 2\tilde{X}_1 + \tilde{K}_{11} & \tilde{K}_{12} \\ \tilde{K}_{12} & 2\tilde{T}_2 + 2\tilde{X}_2 + \tilde{K}_{22} \end{pmatrix}, \tag{30}$$

where

$$\tilde{X}_i = \int d^3 x n_i(\mathbf{x}) \mathbf{x}^2 \tag{31}$$

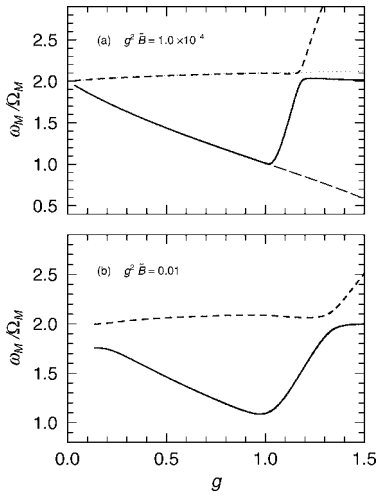

FIG. 5. The frequency of the monopole oscillations, with the external magnetic fields with $g^2\tilde{B} = 1.0\times10^{-4}$ (a) and 1.0×10^{-2} (b). The thick solid and dashed lines represent the results of the out-of-phase and in-phase oscillation modes, respectively. The thin solid and dashed lines denote the results for the out-of-phase and in-phase oscillation modes of the symmetric system, respectively.

$$\tilde{T}_i = \frac{3}{5} \int d^3 x [n_i(\mathbf{x})]^{5/3}, \tag{32}$$

$$\tilde{K}_{11} = -\frac{g}{2} \int d^3 x \left(3n_1 + x \frac{\partial n_1}{\partial x} \right) \left(x \frac{\partial n_2}{\partial x} \right), \tag{33}$$

$$\tilde{K}_{22} = -\frac{g}{2} \int d^3 x \left(x \frac{\partial n_1}{\partial x} \right) \left(3n_2 + x \frac{\partial n_2}{\partial x} \right), \tag{34}$$

$$\begin{aligned} \tilde{K}_{12} &= \frac{g}{2} \int d^3 x \left(3n_1 + x \frac{\partial n_1}{\partial x} \right) \left(3n_2 + x \frac{\partial n_2}{\partial x} \right) \\ &= \frac{g}{2} \int d^3 x \left(x^2 \frac{\partial n_1}{\partial x} \frac{\partial n_2}{\partial x} \right). \end{aligned} \tag{35}$$

In the symmetric system $\rho_1 = \rho_2$ the monopole frequencies are given by $\omega_M^2 = (C_{11} + K_{12})/mX_1$ and $(C_{11} - K_{12})/mX_1$. The eigenvector becomes $\lambda_1 = \lambda_2$ (in-phase) in the respect to the former frequency, and $\lambda_1 = -\lambda_2$ (out-of-phase) in the latter frequency.

In Fig. 5 we show the frequencies of monopole oscillations as functions of the coupling constant g with $g^2\tilde{B} = 1.0\times10^{-4}$ (a) and 1.0×10^{-2} (b). The solid and dashed lines represent the smaller and larger frequencies of two modes, which we call mode-1 and mode-2, respectively.

In Fig. 5(a) we also plot the frequencies of out-of-phase and in-phase modes in the symmetric system without external magnetic field with the thin long-dashed and dotted lines, respectively. The frequencies of the in-phase oscillation in the symmetric system is about $\omega_M \approx 2\Omega_M$, which is the frequency in a noninteracting trapped ideal gas, for any asymmetry. As the coupling constant increases, on the other hand, the frequency of the out-of-phase mode monotonously decreases.

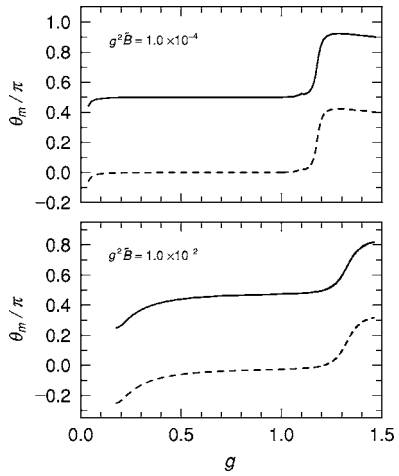

FIG. 6. The mixing angle of the two modes of the monopole oscillation with $g^2\tilde{B}=1.0\times10^{-4}$ (a) and 1.0×10^{-2} (b). The thick solid and dashed lines represent the results of the mode-1 and mode-2, respectively.

In the weak coupling $g\lesssim 1$, the frequencies of the mode-1 and mode-2 are almost the same as those of the in-phase and out-of-phase modes in the symmetric system. As the coupling constant increases, on the other hand, the frequency of the mode-2 rapidly increases above $g\approx 1$. When the coupling constant increases further, the frequency of the out-of-phase mode approaches to that of the in-phase mode, and the level mixing between the two modes occurs. Even after the level mixing, the frequency of the mode-1 increases while the frequency of the mode-2 rarely vary. From those we can suppose that the modes-1 and -2 are almost out-of-phase and in-phase modes, though the two modes are mixed and exchange their roles in strong coupling.

In order to confirm that, here, we calculate the mixing angle θ_m defined as

$$\boldsymbol{\lambda}=\begin{pmatrix}\lambda_1\\ \lambda_2\end{pmatrix}=\frac{1}{\sqrt{2}}\begin{pmatrix}1\\ 1\end{pmatrix}\cos\,\theta_m+\frac{1}{\sqrt{2}}\begin{pmatrix}-1\\ 1\end{pmatrix}\sin\,\theta_m, \qquad (36)$$

where $\boldsymbol{\lambda}$ is an eigenvector obtained from Eq. (28). When $\theta_m=0,\pi$ and $\theta_m=\pi/2$, the modes exhibit the pure in-phase and out-of-phase monopole oscillation of two-component fermions.

In Fig. 6 we show the results with the external magnetic fields $g^2\tilde{B}=1.0\times10^{-4}$ (a) and $g^2\tilde{B}=1.0\times10^{-2}$ (b). In the case of the small magnetic field [Fig. 6(a)], the two modes, the mode-1 and the mode-2, are almost clear out-of-phase and in-phase oscillations before the level mixing. Around $g\approx 1.2$, the modes-1 and -2 are mixed, and the two collective modes exchange their roles in the strong interaction limit. This feature is less clear, but also seen in the case of the strong magnetic field [Fig. 6(b)].

V. SUMMARY

In this paper we study the spin excitation on the dipole and monopole oscillations in the asymmetric two-component fermion condensed system using the scaling method. As for the dipole oscillations the in-phase and the out-of-phase modes are completely decoupled even in the asymmetric system. The two modes can be coupled in the monopole oscillation, but these two modes are rarely mixed except when their frequencies are close.

In all kinds of oscillations the in-phase motions do not have any special behavior even if the two components are largely asymmetric. The frequencies of the in-phase modes are not so different from those of the noninteracting system.

On the other hand, the frequencies of these out-of-phase oscillations monotonously decrease as the repulsive force between the two kinds of fermions becomes larger. As the coupling further increases, the system changes to ferromagnetic and, the frequencies of the out-of-phase oscillations very suddenly increase, though those of the in-phase oscillations do not vary even if the ferromagnetism appears. In addition the frequencies and $M1$ excitation strength show differences between different number asymmetry for $g\gtrsim 1$, where the ferromagnetism appears.

Thus significant information of many-body systems can be obtained only from the out-of-phase oscillations. In this work we describe the two components of fermions with two different spin states. It may be thought to be difficult to establish such experiments at present because we need two kinds of external magnetic fields to control the interaction and the asymmetry. However experimental techniques have been developed, and some new methods making Feshbach resonance without the magnetic field have already been established [17,18]. Hence we expect that experiments will be carried out in the future.

Furthermore a similar work can be done in systems including two different kinds of Fermi gases, where we do not need an external magnetic field to construct the asymmetry. Since the two kinds of fermions cannot be exchanged, we must make a system with their same Fermi energies by changing the numbers of two kinds of fermions at each coupling constant. If we use two kinds of fermions with different masses, we can study a variety of systems.

ACKNOWLEDGMENT

One of the authors (T.M.) thanks the Institute for Nuclear Theory at University of Washington for the hospitality and partial support during the completion of this work.

[1] For reviews, see A. S. Parkins and H. D. F. Walls, Phys. Rep. **303**, 1 (1998); F. Dalfovo, S. Giorgini, L. P. Pitaevskii, and S. Stringari, Rev. Mod. Phys. **71**, 463 (1999); W. Ketterle, D. S. Durfee, and D. M. Stamper-Kum, in *Bose-Einstein Condensation in Atomic Gases*, Proceedings of the International School of Physic "Enrico Fermi," edited by M. Ingusico, S. Stringari, and C. Wieman (IOS Press, Amsterdam, 1999).

[2] E. A. Cornell and C. E. Wieman, Rev. Mod. Phys. **74**, 875 (2002); W. Ketterle, *ibid.* **74**, 1131 (2002).

[3] M. H. Anderson *et al.*, Science **269**, 198 (1995); K. B. Davis M. O. Mewes, M. R. Andrews, N. J. van Druten, D. S. Durfee, D. Mukurn, and W. Ketterle, Phys. Rev. Lett. **75**, 3969 (1995).

[4] B. DeMarco and D. S. Jin, Science **285**, 1703 (1999); S. R. Granade, M. E. Gehm, K. M. OHara, and J. E. Thomas, Phys. Rev. Lett. **88**, 120405 (2002).

[5] A. G. Tuscott, K. E. Strecker, W. I. McAlexander, G. B. Parridge, and R. G. Hullet, Science **291**, 2570 (2001); F. Schreck *et al.*, Phys. Rev. Lett. **87**, 080403 (2001); Z. Hadzibabic *et al.*, *ibid.* **88**, 160401 (2002); **91**, 160401 (2003).

[6] W. Kohn, Phys. Rev. **123**, 1242 (1961).

[7] G. M. Bruun, Phys. Rev. A **63**, 043408 (2001).

[8] K. Goral, M. Brewczyk, and K. Rzazewski, Phys. Rev. A **67**, 025601 (2003).

[9] G. M. Bruun and B. R. Mottelson, Phys. Rev. Lett. **87**, 270403 (2001).

[10] L. Vichi and S. Stringari, Phys. Rev. A **60**, 4734 (1999).

[11] G. F. Bertsch, Nucl. Phys. A **249**, 253 (1975); G. F. Bertsch and K. Stricker, Phys. Rev. C **13**, 1312 (1976); D. M. Brink and Leobardi, Nucl. Phys. A **258**, 285 (1976); T. Suzuki, Prog. Theor. Phys. **64**, 1627 (1980).

[12] O. Bohigas, A. M. Lane, and J. Martorell, Phys. Rep. **51**, 267 (1979).

[13] G. F. Berstch, A. Bulagc, and R. A. Broglia, physics/0403125 (unpublished).

[14] T. Sogo and H. Yabu, Phys. Rev. A **66**, 043611 (2002).

[15] S. D. Gensemer and D. S. Jin, Phys. Rev. Lett. **87**, 173201 (2001).

[16] B. DeMarco and D. S. Jin, Phys. Rev. Lett. **88**, 040405 (2002).

[17] M. Olshanii, Phys. Rev. Lett. **81**, 938 (1998); T. Bergeman, M. G. Moore, and M. Olshanii, *ibid.* **91**, 163201 (2003).

[18] F. K. Fatemi, K. M. Jones, and P. D. Lett, Phys. Rev. Lett. **85**, 4462 (2000); J. M. Gerton, B. J. Frew, and R. G. Hulet, Phys. Rev. A **64**, 053410 (2001).